

Fasudil Attenuates Adriamycin-Induced Cardiac Damage by Modifying Oxidative Stress and Apoptosis Mediated Cellular Signaling

Yi Yan

jiangying people's hospital

Chengyu Xiang

Jiangsu Province Hospital and Nanjing Medical University First Affiliated Hospital

Dingguo Zhang (✉ zhdg0223@126.com)

The first affiliated hospital of Nanjing Medical University <https://orcid.org/0000-0003-0041-6180>

Research Article

Keywords: fasudil, adriamycin, heart injury, apoptosis, senescence, oxidative stress

Posted Date: March 22nd, 2021

DOI: <https://doi.org/10.21203/rs.3.rs-323927/v1>

License:   This work is licensed under a Creative Commons Attribution 4.0 International License.

[Read Full License](#)

Abstract

PURPOSE

To explore the protective mechanism of fasudil, a Rho kinase inhibitor, on acute cardiac injury induced by adriamycin (ADR).

METHODS

In vitro investigations on H9C2 cell line, as well as an in vivo study in a mouse model of ADR-induced acute cardiomyopathy, were performed. In vitro, H9C2 cells were treated with fasudil for 30 mins then incubated with ADR for 24 hours. Cells were collected for immunohistochemistry and western blot study, respectively. In vivo, C57BL6 mice were randomly divided into the following four groups: ADR group; low-dose fasudil (ADR+L); high-dose fasudil (ADR+H); and control group (CON). Animals were injected i.p. 20 mg/kg ADR once in group ADR. And animals were injected i.p. fasudil (2 or 10 mg/kg/day) daily once for six times in group ADR+L and ADR+H, respectively. Blood samples and heart tissues were collected for assays.

RESULTS

In vitro, fasudil treatment ameliorated ADR-induced immunofluorescence reaction of 8-OHdG, decreased the expression of TUNEL cells and protein of Bax, Caspase-3 and p53, and increased the expression of protein of Bcl-2 and SIRT 1. In the mouse model, administration of fasudil significantly ameliorated ADR-induced cardiac damage, suppressed cell apoptosis and senescence, ameliorated redox imbalance and DNA damage.

CONCLUSION

Fasudil has the protective effect on adriamycin induced acute cardiotoxicity, which is partially attributed to its antioxidant, anti-senescence, and anti-apoptotic effects of inhibiting the RhoA/Rho kinase signaling pathway.

1 Introduction

Adriamycin (ADR) or doxorubicin, one of anthracycline antibiotics, is an effective antitumor agent successfully to treat hematopoietic and solid tumors [1, 2]. However, its clinical utility is limited due to acute and chronic toxicities, particularly cardiotoxicity [3, 4]. Acute cardiotoxicity is more common than previously thought and predicts poor outcomes. Acute cardiotoxicity starts within 24 h of the infusion and occurs in up to 40% of the patient population [7]. Therefore, effective cardioprotective adjuvants to minimize the ADR-induced acute cardiotoxicity are urgently needed.

The mechanisms responsible are multifactorial and remain enigmatic [5], including oxidative stress, mitochondrial dysfunction, intracellular calcium overload, myofibrillar degeneration, cytokine release, and

induction of cardiomyocyte apoptosis[6–8]. Among these mechanisms, oxidative stress and apoptosis appear to be the main triggers of this drug-induced cardiotoxicity[9, 10]. However, it has recently been suggested that senescence may be another mechanism of cardiotoxicity induced by ADR[11]. Cellular senescence is a fundamental cellular program which is characterized by a series of morphological and physiological changes including irreversible block of proliferation. In addition, it contributes to the physiology of living tissues, the aging process, and age-related diseases as cancer, diabetes, osteoporosis, and cardiovascular and neurodegenerative diseases [12, 13].

Fasudil, a drug that inhibits ROCK receptor, is widely used to prevent cerebral vasospasm and cerebral ischemia after subarachnoid hemorrhage in clinical practice [14]. In our previous study, we found fasudil has antioxidant, anti-inflammatory and anti-apoptotic effects in contrast-induced acute kidney injury model [20]. Recently, we also demonstrated that fasudil could attenuated ADR-induced chronic cardiotoxicity, which is in line with the previous study [3, 19]. Still more, many studies have indicated this drug is a crucial regulator of both cardiac function and tumorigenesis[15]. And plenty of animal models have demonstrated the cardio-protective effects of fasudil, including myocardial ischemia/reperfusion injury, pressure overload-induced heart failure and ischemic hypercholesterolemic heart[16–18]. However, it is not known whether inhibition of Rho-kinase could alleviate the acute heart injury induced by ADR. In this study, we aimed to study the effects of ROCK inhibition by fasudil on acute heart injury induced by ADR in vitro and in vivo .

2 Materials And Methods

2.1 In vivo mouse model of ADR-induced acute cardiotoxicity

Male C57BL6 mice (Laboratory Animal Services Centre, Nanjing Medical University, Nanjing) at 6 to 8 weeks of age were randomly classified into 4 groups: ADR group; low-dose fasudil (ADR + L); high-dose fasudil (ADR + H); and control group (CON). Animals were injected i.p 20 mg/kg ADR once in group ADR. And animals were injected i.p fasudil (2 or 10 mg/kg/day) daily once for six times in group L and H. Control group received only normal saline. Before each injection, the animal's weight was taken and the dose was recalculated. All animals are treated in accordance with the approved program and animal welfare regulations for Animal Care and Use Committee of the Nanjing Medical University.

Twenty four hours after the last injection, the animals were weighed and euthanized. Blood samples were collected for biochemical assays. Hearts were collected, washed with phosphate buffer saline (PBS) and weighed. Rapid dissection of cardiac tissue; rapid freezing of a portion of the left ventricle (LV) in liquid nitrogen and then preserved at –80°C for protein analysis. The other part was preserved in 10% paraformaldehyde for histopathological and immunohistochemical analysis.

2.2 In vitro model of ADR-induced cardiotoxicity

H9C2 cells were maintained in Iscove's modified Dulbecco's medium supplemented with 10% fetal calf serum and cultured in 5% CO₂ at 37°C.

Cells were seeded at 2×10^4 cells per well (6 well plates) for 24 hours and then incubated with or without fasudil (10uM or 20uM). After 30 minutes, ADR(1uM) was added to the system for another 24 hours. Then cells of different treatment groups were collected for analysis.

2.3 Measurement of plasma enzyme, oxidative marker serum lactate dehydrogenase (LDH) and creatine phosphokinase (CK) levels

The levels of LDH and CK in plasma and cell suspension after different treatments were detected with the commercial assay kits(Nanjing Jiancheng Bioengineering Institute, Nanjing, China)according to manufacturer's instructions. The cardiac tissue levels of superoxide dismutase (SOD) and lipid peroxidation: malondialdehyde (MDA) were monitored in 10% PBS tissue homogenate according to manufacturer's instructions(Nanjing Jiancheng Bioengineering Institute, Nanjing, China).

2.4 Histopathological examination

The heart tissue of mice was fixed in 10% paraformaldehyde for 48 hours and routinely embedded in paraffin. Morphological changes of myocardial injury were observed by hematoxylin-eosin (HE) staining and total collagen (T-col) observed by Sirius red staining in paraffin-embedded sections (5 micron thick) under a light microscope, respectively.

2.5 Immunohistochemistry for β -gal

After deparaffinization, the heart sections were washed with PBS, incubated with 3% H₂O₂ for 30 min, then blocked with 10% goat serum for 1hour to prevent nonspecific staining and overnight incubated with primary antibody (Anti-beta Galactosidase(β -gal), 1:1000,Abcam, UK)at 4°C. Tissues were washed and incubated with the appropriate secondary antibody at 37°C for 1 hour, and the positive cells were observed using Vector Impress Kit (Impress Kit, Vector Laboratories; Burlingame, CA).

2.6 Immunofluorescence for 8-OHdG

Paraffin sections were deparaffinized in xylene and rehydrated in alcohol gradient. Cells were inoculated on cell slides fixed with paraformaldehyde for 15 minutes then washed the excess paraformaldehyde with PBS. H₂O₂ solution(3%) was dropped on slides for 10 minutes then washed with PBS. After 30 minutes of blocking with 10% goat serum, sections were incubated overnight with diluted primary antibody (Anti- DNA/RNA Damage antibody(8-OHdG), 1:1000,Abcam, UK)at 4°C. Fluorescein isothiocyanate-conjugated secondary antibody was then used for detecting the binding sites of the primary antibody, and the samples were observed by fluorescence microscope.

2.7 Terminal Deoxynucleotidyltransferase–Mediated Nick-End Labeling Assay(TUNEL)

Cells of different treatment groups were collected, then fixed the cells with paraformaldehyde for 15 minutes and permeated with Proteinase K for 15 minutes, after washed with PBS twice, cell slides were incubated with TUNEL reaction mixture for 1 hour, the nucleus was stained with DAPI in a dark room for 10 minutes. Finally, the positive cells were observed and photographed under a fluorescent inverted microscope.

2.8 Western Blot

Proteins were extracted from heart tissues and cells, quantitated using a protein assay kit. Equal amount of protein was loaded and proteins were separated by SDS-PAGE and electrophoretically transferred to nitrocellulose membranes. Membranes were blocked with 5% PBS milk for 1 hour, and then incubated with primary antibody at 4°C overnight. After incubation with the primary antibody, the bound antibody was visualized with horseradish peroxidase-coupled secondary antibodies and chemiluminescence developing agents. Following antibodies were used in the research :ROCK1, ROCK2, MYPT (1:500,Bioworld Technology ,China); p53, Bcl-2 (1:500,Santa Cruz Biotechnology, USA); Bax(1:500,Abcam,UK); NF-κB,caspase-3(1:1000,CST,USA);

SIRT1,Foxo3(1:1000,Abcam,UK);superoxide dismutase 1 (SOD1) (1:2000,CST,USA) ;superoxide dismutase 2 (SOD2)(1 : 1000, Abcam, UK) andβ-actin(1:2000,Abcam,UK).

2.9 Statistical analysis

The data were expressed as mean ± standard deviation and analyzed by the one-way analysis of variance (ANOVA) and Bonferroni multiple-range test. $P < 0.05$ was considered to have statistical significance.

3 Results

3.1 Fasudil ameliorated ADR-induced body weight changes and survival rate

On the first day of the experiment, no significant differences in the body weight among the groups were found. However, after administered with ADR, the body weight of mice significantly decreased ($P < 0.001$); the body weights of mice in the control group were increased along with prolonging of feeding period (Table 1). Three days after adriamycin treatment, survival was significantly lower in ADR compared with CON mice (60%VS 100%). Fasudil treatment improve the survival rate of mice (ADR + L,80%;ADR + H,100%) (Fig. 1).

3.2 Fasudil attenuated ADR-induced myocardial injury

The mice were challenged with ADR, which caused marked myocardial tissue damage as evidenced by elevated serum creatine kinase (CK) and lactate dehydrogenase (LDH). Fasudil treatment significantly reduced ADR-induced elevation of LDH and CK in the mice (Table 2). Similar results were obtained in cell experiments.(Table 3)General morphology of cardiac tissues were observed by HE staining, and we found

that myocardial cells of ADR injection group showed irregular shape, myocardial fibers disarrangement, muscle fiber fracture, and inflammatory cell infiltration. At the same time myocardial cell of CON group had normal size and morphology, cardiac myocytes were regularly shaped, muscle fibers arranged in neat, the cytoplasm and nuclear stained uniform (Fig. 2). The T-Col staining showed an increased proportion of collagen accumulated in interstitial space in the heart of ADR-treated mice. (Fig. 2) However, after the intervention of fasudil, the cardiomyocytes vacuolization and irregular cardiomyocytes alignment were attenuated, and the protective effect of fasudil was dose dependent.

2.3 Fasudil inhibited ADR-induced cellular DNA damage

DNA damage of cardiomyocytes was evaluated by performing immunofluorescence in vivo and in vitro, respectively. The immunofluorescence reaction of 8-OHdG in control group was moderate, while that of 8-OHdG in ADR group was severe. However, the immunofluorescence reaction of 8-OHdG decreased with the use of fasudil, although exposed to ADR, especially when high dose fasudil was administrated ($P < 0.001$). (Fig. 3A) Similar results were obtained in H9C2 cell experiments. In vitro, fasudil treatment suppressed the immunofluorescence reaction of 8-OHdG induced by ADR(Fig. 3B).

3.4 Fasudil inhibited ADR-induced cellular apoptosis

In vitro, the levels of apoptosis detected by TUNEL staining were increased after ADR treatment, while fasudil has a protective effect on apoptosis induced by ADR, which is dose-dependent. (Fig. 4A) The expression of apoptosis-related factors protein in all groups were detected through western blot. A dramatic decrease of Bcl-2 in the ADR group was found when compared with the CON group ($p < 0.001$). However, a significantly increase of the expressions of pro-apoptotic factors such as Bax, Caspase-3, in the ADR group were found when compared with CON group. After fasudil was administered, these apoptosis related indexes expressions decreased (Fig. 4B). Similar results were obtained in vivo. In mouse model of ADR-induced cardiotoxicity, fasudil treatment suppressed the Bax and Caspase-3 expression, while enhanced the expression of Bcl-2 significantly (Fig. 4C).

3.5 Fasudil inhibited ADR-induced cellular senescence

Cellular senescence was confirmed by β -gal assay. β -gal assay of control and treated groups showed that while ADR induced senescence in myocardium as evidenced by presence of significant number of β -gal positive cells. Fasudil pretreated animals were significantly protected from ADR-induced cellular senescence as evidenced by the decrease in β -gal positive cells in mice contreated with ADR and fasudil(Fig. 5A). In order to delineate the molecular basis of ADR-induced cellular senescence and the protective effect of fasudil, we next examined the levels of senescence regulators in protein lysates prepared from control, ADR alone and ADR plus fasudil treated animals by Western blot. Data showed that ADR significantly reduced the expression of SIRT1 while increased the levels of senescence inducers Foxo3, p53 and NF- κ B. Most importantly, treatment with fasudil inhibited the expression levels of Foxo3 and NF- κ B, and increase the expression level of SIRT1, especially with high dose fasudil. (Fig. 5B) Similar

results were obtained in H9C2 cell experiments. In vitro, fasudil treatment suppressed the expression levels of p53, while increased the expression level of SIRT1 induced by ADR(Fig. 5C).

3.6 Fasudil alleviated ADR-induced oxidative stress reaction

A rise in intracellular reactive oxygen species (ROS) is accompanied with the process of senescence and apoptosis. Several endogenous enzymes including catalase, glutathione peroxidase, superoxide dismutase (SOD) are involved in protection of ROS-induced cellular damage. The cardiac enzymatic activities of total SOD and MDA contents were measured in vivo. As shown in Table 4, the activities of SOD decreased significantly and MDA contents increased significantly in mice treated with ADR compared with that in the CON group ($P < 0.001$). High doses of fasudil had protective effects to reduce oxidative stress levels. The expression of SOD1 and SOD2 tested by Western blot further demonstrated that ADR decrease the anti-oxidative stress levels while fasudil administration could increase the anti-oxidative stress levels. (Fig. 6)

3.7 Fasudil inhibited ADR-induced ROCK signaling pathway changes

In order to study the effect of Rho kinase on ADR-induced cardiac injury, the expression of ROCK1 and 2, the main Rho kinase proteins, were examined in vivo. As shown in Fig. 7, the levels of ROCK1 and ROCK2 increased significantly after ADR application ($p < 0.01$), whereas the levels of ADR + L and ADR + H groups decrease remarkably ($p < 0.01$). As expected, MYPT-1 (a Rho kinase specific effector) level in ADR group was remarkably higher than that in CON group ($p < 0.001$). And fasudil reduced the level of the MYPT-1 protein in comparison with the ADR group ($p < 0.001$).

4. Discussion

The aim of this study was to investigate the role of fasudil in prevention of cardiac dysfunction and biochemical changes in acute doxorubicin-induced cardiotoxicity. Present study demonstrated the efficacy of fasudil in reducing acute cardiotoxicity in in vitro models of H9C2 cell line and in the in vivo model of mice. In addition, our findings show that fasudil suppressed heart oxidative stress, reduce DNA damage of cardiac cells, thereby blocking cellular senescence and inhibiting apoptosis.

Whole-body wasting is shown to be an independent risk factor for mortality in heart failure[21]. In present study, doxorubicin-injected animals weighed significantly lesser than their controls, which is in agreement with reported data [5]. As a consequence of acute heart injury, survival was lower remarkably in ADR mice than that of CON mice. Administration of fasudil increased the survival of ADR treated mice and the protection of fasudil was dose-dependent. Collagen contents in the heart tissues were significantly increased in the ADR group, which may lead heart stiffness and dysfunction. Fasudil reduced collagen aggregation and myocardial fibrosis caused by ADR.

The activities of serum CK and LDH have been widely used as parameters for the diagnosis of cardiac injury [22, 23]. In this study, the elevated serum CK and LDH in ADR-injected animals are suggestive of the deleterious effects of doxorubicin on cardiomyocytes. Administration of fasudil especially high dose fasudil protected the myocardium as evidenced by the reduction in the leakage of CK and LDH into the circulation. Similarly, in vitro experiments, the levels of CK and LDH were significantly increased in ADR-treated cardiomyocytes, and decreased after fasudil treatment.

It is now well recognized that increased ROS generation is the pivotal point upstream of the mechanisms associated with ADR-induced cardiotoxicity. ROS can cause lipid peroxidation, disrupt cell membrane functions and trigger cellular senescence [24, 25]. Increasing evidence indicated that senescence takes part in anthracycline-driven cardiotoxic effects, affecting the functional activity of cardiomyocytes and other cardiac cells. Therefore, decreasing oxidative damage might counteract the manifestations of cardiotoxicity. SOD is a ubiquitous family of enzymes with the function of eliminating ROS. MDA is a peroxide product of polyunsaturated fatty acid and a scientifically recognized oxidative stress index [26]. Previous studies have indicated that ADR could inhibit the SOD enzyme activities. ADR-induced heart injury is strongly linked to an increase in generation of ROS and antioxidant depletion in cardiac tissue [27]. RhoA/ROCK pathway was reported to participate in the regulation of oxidative stress. Previous studies have shown that the activation of ROCK can increase the level of oxidative stress [28, 29]. MDA increased while SOD decreased in ADR-treated mice, fasudil alleviated the oxidative damage caused by ADR, as evident from the present study. This indicated that RhoA/ROCK pathway can up-regulate antioxidant enzymes to reduce oxidative stress levels. In line with the increased oxidative stress reaction, ADR induced notable senescence in myocardium as evidenced by presence of significant number of β -gal positive cells. SIRT1/Foxo3 axis played an important role in cellular senescence. SIRT1 inhibited cellular damage and senescence by blocking the activities of Foxo3 [30, 31]. Moreover, activation of SIRT1, Foxo3, NF- κ B and p53 taking part in senescence changes in myocytes have been demonstrated in many models [32–34]. In present study, the expression of NF- κ B and p53 were markedly elevated in ADR group when compared with control group. However, inhibition of RhoA/ROCK pathway by fasudil leads to fewer senescence. Administration of fasudil, especially high dose fasudil, produced lower levels of β -gal, Foxo3, NF- κ B and p53 when compared with ADR group.

Some studies have also shown that the oxidative stress evoked by ADR activates apoptotic signaling leading to cardiomyocyte damage and apoptosis [35, 36]. Apoptosis has been implicated in cardiac injury evoked by ADR [8, 37]. And, RhoA/ROCK pathway appears to play an important role in myocardial apoptosis [38]. In present study, the expression of ROCK1, ROCK2 and MYPT1 proteins were increased after ADR administration. We found that both low and high doses of fasudil inhibited the expression of ROCK1, ROCK2 and MYPT1, suggesting that the reduction of ROCK activity by this drug may contribute to the reduction of apoptosis. The Bcl-2 family of proteins is a major group of regulators of the mitochondrial pathway of apoptosis [39]. ADR breaks the balance between Bax and Bcl-2, increasing the expression of Bax and decreasing Bcl-2 at the same time, which leads to apoptosis [40, 41]. Moreover, activation of Caspase-3 takes part in the ADR-induced apoptotic changes in myocytes [42].

8-OHdG is a marker of DNA damage, the accumulation of DNA damage eventually accelerated apoptosis of myocytes[43]. We assessed the level of apoptosis after ADR treatment by detecting the immunofluorescence reactions of 8-OHdG. The results showed that either in vivo or in vitro, 8-OHdG in control group was moderate, while that of 8-OHdG in ADR group was severe. However, the immunofluorescence reaction of 8-OHdG decreased with the use of fasudil, although exposed to ADR, especially when high dose fasudil was administered. The results of TUNEL staining also confirmed that fasudil can reduce the apoptosis caused by ADR in vitro.

Our findings revealed that a variety of pathways activation contributes to ADR-induced myocardial cell apoptosis. However, a notable reduction in ADR-induced cellular apoptosis in response to fasudil was observed. Therefore, preventing the activation of ADR-induced apoptosis-related protein might be an additional mechanism of fasudil to avoid cell apoptosis.

3. Conclusion

In conclusion, using in vitro model of H9C2 cell line and in vivo mouse model of ADR-induced cardiotoxicity, we demonstrated the protective effects of fasudil against ADR-induced cardiotoxicity, possibly mediated through suppression of oxidative stress, apoptosis and senescence. The results indicated that RhoA/ROCK pathway inhibitors, fasudil, may have important potential in the treatment of ADR induced cardiotoxicity in clinical.

Declarations

Author contributions

DZ conceived and designed the experiments; YY and CY performed the experiments; YY and DZ wrote the manuscript. All authors read and approved the final manuscript.

Data availability

Not applicable.

Conflict of interests

The authors declare that there are no conflicts of interests.

Ethics Approval This study was approved by the Animal Protection and Use Committee of Nanjing Medical University and was performed according to the Chinese guidelines for animal welfare.

References

[1] Nozaki N, Shishido T, Takeishi Y, Kubota I. Modulation of doxorubicin-induced cardiac dysfunction in toll-like receptor-2-knockout mice *Circulation* 2004,110(18):2869-74.

- [2] Zakaria N, Khalil SR, Awad A, Khairy GM. Quercetin Reverses Altered Energy Metabolism in the Heart of Rats Receiving Adriamycin Chemotherapy Cardiovascular toxicology 2018,18(2):109-19.
- [3] Wang N, Guan P, Zhang JP, Chang YZ, Gu LJ, Hao FK, Shi ZH, Wang FY, Chu L. Preventive effects of fasudil on adriamycin-induced cardiomyopathy: possible involvement of inhibition of RhoA/ROCK pathway Food and chemical toxicology : an international journal published for the British Industrial Biological Research Association 2011,49(11):2975-82.
- [4] Bose C, Awasthi S, Sharma R, Benes H, Hauer-Jensen M, Boerma M, Singh SP. Sulforaphane potentiates anticancer effects of doxorubicin and attenuates its cardiotoxicity in a breast cancer model PloS one 2018,13(3):e0193918.
- [5] Thandavarayan RA, Watanabe K, Sari FR, Ma M, Lakshmanan AP, Giridharan VV, Gurusamy N, Nishida H, Konishi T, Zhang S, Muslin AJ, Kodama M, Aizawa Y. Modulation of doxorubicin-induced cardiac dysfunction in dominant-negative p38alpha mitogen-activated protein kinase mice Free radical biology & medicine 2010,49(9):1422-31.
- [6] Dai GF, Wang Z, Zhang JY. Octreotide protects doxorubicin-induced cardiac toxicity via regulating oxidative stress European review for medical and pharmacological sciences 2018,22(18):6139-48.
- [7] Octavia Y, Tocchetti CG, Gabrielson KL, Janssens S, Crijns HJ, Moens AL. Doxorubicin-induced cardiomyopathy: from molecular mechanisms to therapeutic strategies Journal of molecular and cellular cardiology 2012,52(6):1213-25.
- [8] Xia P, Liu Y, Chen J, Coates S, Liu D, Cheng Z. Inhibition of cyclin-dependent kinase 2 protects against doxorubicin-induced cardiomyocyte apoptosis and cardiomyopathy The Journal of biological chemistry 2018.
- [9] Li T, Singal PK. Adriamycin-induced early changes in myocardial antioxidant enzymes and their modulation by probucol Circulation 2000,102(17):2105-10.
- [10] Pereira GC, Silva AM, Diogo CV, Carvalho FS, Monteiro P, Oliveira PJ. Drug-induced cardiac mitochondrial toxicity and protection: from doxorubicin to carvedilol Current pharmaceutical design 2011,17(20):2113-29.
- [11] Fang J, Tang Y, Cheng X, Wang L, Cai C, Zhang X, Liu S, Li P. Exenatide alleviates adriamycin-induced heart dysfunction in mice: Modulation of oxidative stress, apoptosis and inflammation Chemicobiological interactions 2019,304:186-93.
- [12] Sung JY, Lee KY, Kim JR, Choi HC. Interaction between mTOR pathway inhibition and autophagy induction attenuates adriamycin-induced vascular smooth muscle cell senescence through decreased expressions of p53/p21/p16 Experimental gerontology 2018,109:51-8.

- [13] You R, Dai J, Zhang P, Barding GA, Jr., Raftery D. Dynamic Metabolic Response to Adriamycin-Induced Senescence in Breast Cancer Cells *Metabolites*2018,8(4).
- [14] Song X, He R, Han W, Li T, Xie L, Cheng L, Chen H, Xie M, Jiang L. Protective effects of the ROCK inhibitor fasudil against cognitive dysfunction following status epilepticus in male rats *Journal of neuroscience research*2018.
- [15] Zhao Y, Zhang Y, Vazirinejad Mehdiabad M, Zhou K, Chen Y, Li L, Guo J, Xu C. Enhanced anti-tumor effect of liposomal Fasudil on hepatocellular carcinoma in vitro and in vivo *PLoS one*2019,14(10):e0223232.
- [16] Huang YY, Wu JM, Su T, Zhang SY, Lin XJ. Fasudil, a Rho-Kinase Inhibitor, Exerts Cardioprotective Function in Animal Models of Myocardial Ischemia/Reperfusion Injury: A Meta-Analysis and Review of Preclinical Evidence and Possible Mechanisms *Frontiers in pharmacology*2018,9:1083.
- [17] Guan P, Liang Y, Wang N. Fasudil alleviates pressure overload-induced heart failure by activating Nrf2-mediated antioxidant responses *Journal of cellular biochemistry*2018,119(8):6452-60.
- [18] Wu N, Li W, Shu W, Lv Y, Jia D. Inhibition of Rho-kinase by fasudil restores the cardioprotection of ischemic postconditioning in hypercholesterolemic rat heart *Molecular medicine reports*2014,10(5):2517-24.
- [19] Yan Y, Xiang C, Yang Z, Miao D, Zhang D. Rho Kinase Inhibition by Fasudil Attenuates Adriamycin-Induced Chronic Heart Injury *Cardiovascular toxicology*2020.
- [20] Wang Y, Zhang H, Yang Z, Miao D, Zhang D. Rho Kinase Inhibitor, Fasudil, Attenuates Contrast-induced Acute Kidney Injury *Basic & clinical pharmacology & toxicology*2018,122(2):278-87.
- [21] Anker SD, Ponikowski P, Varney S, Chua TP, Clark AL, Webb-Peploe KM, Harrington D, Kox WJ, Poole-Wilson PA, Coats AJ. Wasting as independent risk factor for mortality in chronic heart failure *Lancet*1997,349(9058):1050-3.
- [22] El-Boghdady NA. Increased cardiac endothelin-1 and nitric oxide in adriamycin-induced acute cardiotoxicity: protective effect of Ginkgo biloba extract *Indian journal of biochemistry & biophysics*2013,50(3):202-9.
- [23] Mohamad RH, El-Bastawesy AM, Zekry ZK, Al-Mehdar HA, Al-Said MG, Aly SS, Sharawy SM, El-Merzabani MM. The role of Curcuma longa against doxorubicin (adriamycin)-induced toxicity in rats *Journal of medicinal food*2009,12(2):394-402.
- [24] Liu ML, Wang ML, Lv JJ, Wei J, Wan J. Glibenclamide exacerbates adriamycin-induced cardiotoxicity by activating oxidative stress-induced endoplasmic reticulum stress in rats *Exp Ther Med*2018,15(4):3425-31.

- [25] Aniss HA, Said Ael M, El Sayed IH, Adly C. Amelioration of adriamycin-induced cardiotoxicity by Salsola kali aqueous extract is mediated by lowering oxidative stress Redox report : communications in free radical research 2014,19(4):170-8.
- [26] Del Rio D, Stewart AJ, Pellegrini N. A review of recent studies on malondialdehyde as toxic molecule and biological marker of oxidative stress Nutrition, metabolism, and cardiovascular diseases : NMCD 2005,15(4):316-28.
- [27] Ozdogan K, Taskin E, Dursun N. Protective effect of carnosine on adriamycin-induced oxidative heart damage in rats Anadolu kardiyoloji dergisi : AKD = the Anatolian journal of cardiology 2011,11(1):3-10.
- [28] Zhang XH, Feng ZH, Wang XY. The ROCK pathway inhibitor Y-27632 mitigates hypoxia and oxidative stress-induced injury to retinal Muller cells Neural regeneration research 2018,13(3):549-55.
- [29] Liang J, Zeng X, Halifu Y, Chen W, Hu F, Wang P, Zhang H, Kang X. Blocking RhoA/ROCK inhibits the pathogenesis of pemphigus vulgaris by suppressing oxidative stress and apoptosis through TAK1/NOD2-mediated NF-kappaB pathway Molecular and cellular biochemistry 2017,436(1-2):151-8.
- [30] Lee D, Goldberg AL. SIRT1 protein, by blocking the activities of transcription factors FoxO1 and FoxO3, inhibits muscle atrophy and promotes muscle growth The Journal of biological chemistry 2013,288(42):30515-26.
- [31] Lin CH, Lin CC, Ting WJ, Pai PY, Kuo CH, Ho TJ, Kuo WW, Chang CH, Huang CY, Lin WT. Resveratrol enhanced FOXO3 phosphorylation via synergetic activation of SIRT1 and PI3K/Akt signaling to improve the effects of exercise in elderly rat hearts Age 2014,36(5):9705.
- [32] Oka S, Alcendor R, Zhai P, Park JY, Shao D, Cho J, Yamamoto T, Tian B, Sadoshima J. PPARalpha-Sirt1 complex mediates cardiac hypertrophy and failure through suppression of the ERR transcriptional pathway Cell metabolism 2011,14(5):598-611.
- [33] Guo RM, Xu WM, Lin JC, Mo LQ, Hua XX, Chen PX, Wu K, Zheng DD, Feng JQ. Activation of the p38 MAPK/NF-kappaB pathway contributes to doxorubicin-induced inflammation and cytotoxicity in H9c2 cardiac cells Molecular medicine reports 2013,8(2):603-8.
- [34] Kannappan R, Mattapally S, Wagle PA, Zhang J. Transactivation domain of p53 regulates DNA repair and integrity in human iPS cells American journal of physiology Heart and circulatory physiology 2018,315(3):H512-H21.
- [35] He L, Xiao J, Fu H, Du G, Xiao X, Zhang C, Gu Y, Ma Y. Effect of oxidative stress on ventricular arrhythmia in rabbits with adriamycin-induced cardiomyopathy Journal of Huazhong University of Science and Technology Medical sciences = Hua zhong ke ji da xue xue bao Yi xue Ying De wen ban = Huazhong keji daxue xuebao Yixue Yingdewen ban 2012,32(3):334-9.

- [36] Abd El-Aziz TA, Mohamed RH, Pasha HF, Abdel-Aziz HR. Catechin protects against oxidative stress and inflammatory-mediated cardiotoxicity in adriamycin-treated rats *Clinical and experimental medicine*2012,12(4):233-40.
- [37] Preau S, Delguste F, Yu Y, Remy-Jouet I, Richard V, Saulnier F, Boulanger E, Neviere R. Endotoxemia Engages the RhoA Kinase Pathway to Impair Cardiac Function By Altering Cytoskeleton, Mitochondrial Fission, and Autophagy *Antioxidants & redox signaling*2016,24(10):529-42.
- [38] Hattori T, Shimokawa H, Higashi M, Hiroki J, Mukai Y, Tsutsui H, Kaibuchi K, Takeshita A. Long-term inhibition of Rho-kinase suppresses left ventricular remodeling after myocardial infarction in mice *Circulation*2004,109(18):2234-9.
- [39] Lv X, Yu X, Wang Y, Wang F, Li H, Wang Y, Lu D, Qi R, Wang H. Berberine inhibits doxorubicin-triggered cardiomyocyte apoptosis via attenuating mitochondrial dysfunction and increasing Bcl-2 expression *PLoS one*2012,7(10):e47351.
- [40] Childs AC, Phaneuf SL, Dirks AJ, Phillips T, Leeuwenburgh C. Doxorubicin treatment in vivo causes cytochrome C release and cardiomyocyte apoptosis, as well as increased mitochondrial efficiency, superoxide dismutase activity, and Bcl-2:Bax ratio *Cancer research*2002,62(16):4592-8.
- [41] Jing X, Yang J, Jiang L, Chen J, Wang H. MicroRNA-29b Regulates the Mitochondria-Dependent Apoptotic Pathway by Targeting Bax in Doxorubicin Cardiotoxicity *Cellular physiology and biochemistry : international journal of experimental cellular physiology, biochemistry, and pharmacology*2018,48(2):692-704.
- [42] Bao YL, Wang Y, Wu Z, Cui XX, Du JJ, Wang YL, Zhao M. Effects of caspase inhibitor z-VAD-fmk on the expressions of calumenin, caspase-3, GRP78 and GRP94 in adriamycin-injured cardiomyocytes *Zhongguo ying yong sheng li xue za zhi = Zhongguo yingyong shenglixue zazhi = Chinese journal of applied physiology*2017,33(3):222-5.
- [43] Yanagi S, Matsumura K, Marui A, Morishima M, Hyon SH, Ikeda T, Sakata R. Oral pretreatment with a green tea polyphenol for cardioprotection against ischemia-reperfusion injury in an isolated rat heart model *The Journal of thoracic and cardiovascular surgery*2011,141(2):511-7.

Tables

Table1 Body weight changes of each group

Day	CON	ADR	ADR+L	ADR+H
1	17.97±0.65	18.06±0.56	18.03±0.68	18.04±0.71
2	18.06±0.59	18.16±0.62	18.10±0.60	18.02±0.84
3	18.25±0.63	18.26±0.67	18.23±0.49	18.26±0.79
4 (ADR injection)	18.36±0.56	18.40±0.59	18.50±0.42	18.68±0.67
5	18.40±0.62	17.78±0.69*	17.72±0.43*	17.85±0.71
6	18.61±0.51	16.96±0.67***	16.91±0.35***	17.14±0.69***
7	18.83±0.60	16.14±0.61***	16.05±0.48***	16.38±0.59***

*P<0.05, ***P<0.001 compared to CON group

Table 2 LDH and CK levels of each group in vivo

Group	LDH(U/L)	CK(U/L)
CON	1740.48±159.09	179.81±60.23
ADR	3193.37±273.66***	810.79±129.57***
ADR+L	3102.31±332.96***	607.16±114.07*** ##
ADR+H	2790.54±347.08*** ##	507.16±139.77*** ##

***P<0.001 compared to CON group; ##P<0.01 compared to ADR group

Table 3 LDH and CK levels of each group in vitro

Group	LDH(U/L)	CK(U/L)
CON	102.68±10.35	159.32±38.84
ADR	162.89±33.31**	459.76±62.62***
ADR+L	137.32±38.81	362.93±69.82*** #
ADR+H	112.99±11.61 [#]	318.23±43.86*** ##

P<0.01, *P<0.001 compared to CON group; #P<0.05, ##P<0.01

Table 4 SOD and MDA levels of each group

Group	SOD(U/mg protein)	MDA(nmol/mg protein)
CON	160.62±13.72	15.61±1.73
ADR	75.70±9.42***	29.79±1.81***
ADR+L	102.84±13.89*** ###	26.84±2.37*** #
ADR+H	120.34±14.30*** ### &	20.96±1.86*** ### &&&

***P<0.001 compared to CON group; ##P<0.01, ###P<0.001 compared to ADR group; &P<0.05, &&&P<0.001 compared to ADR+L group.

Figures

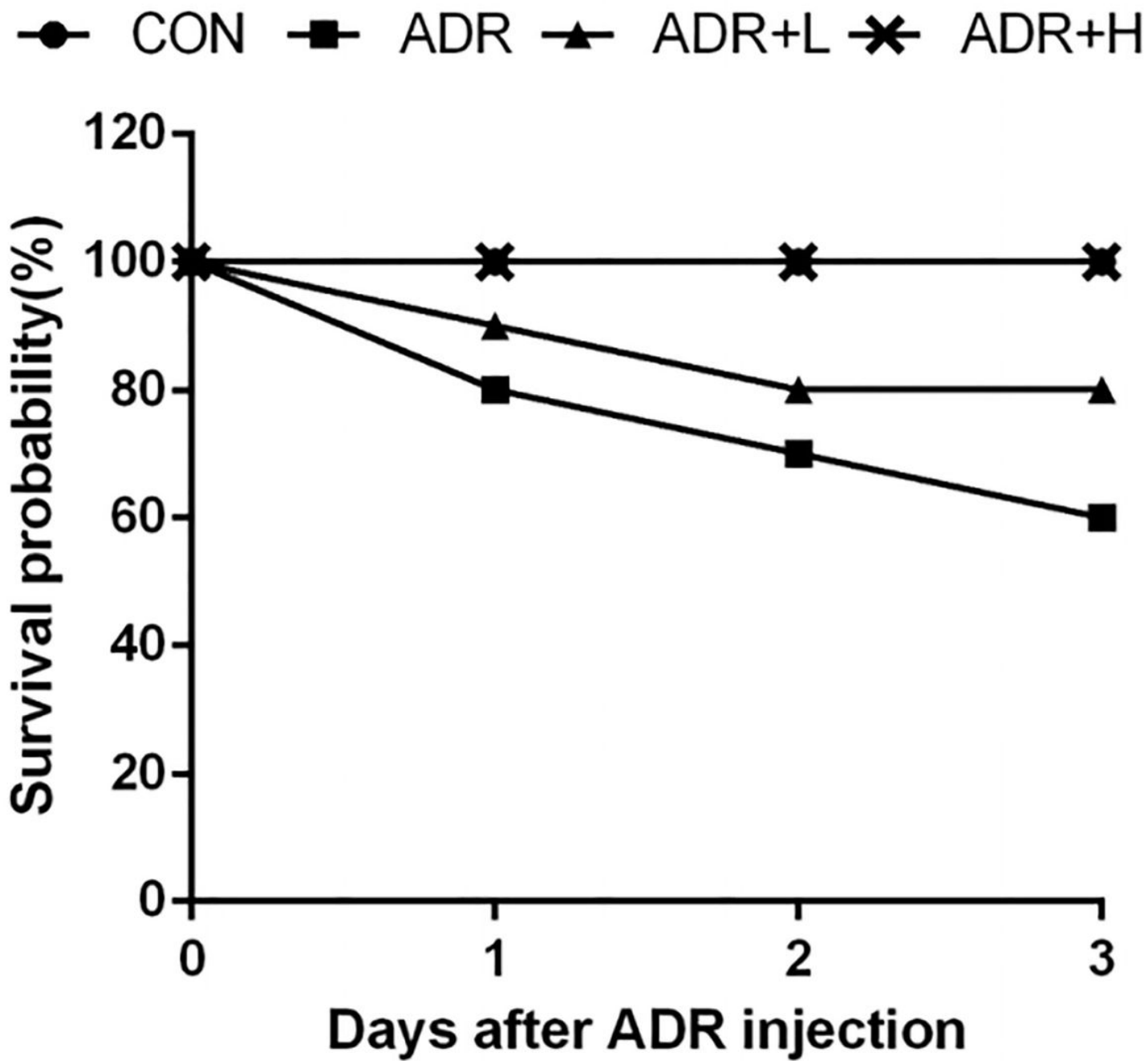


Figure 1

Survival rate of each group(n=10,each). CON group 100%; ADR group 60%; ADR+L group 80%; ADR+H group 100%.

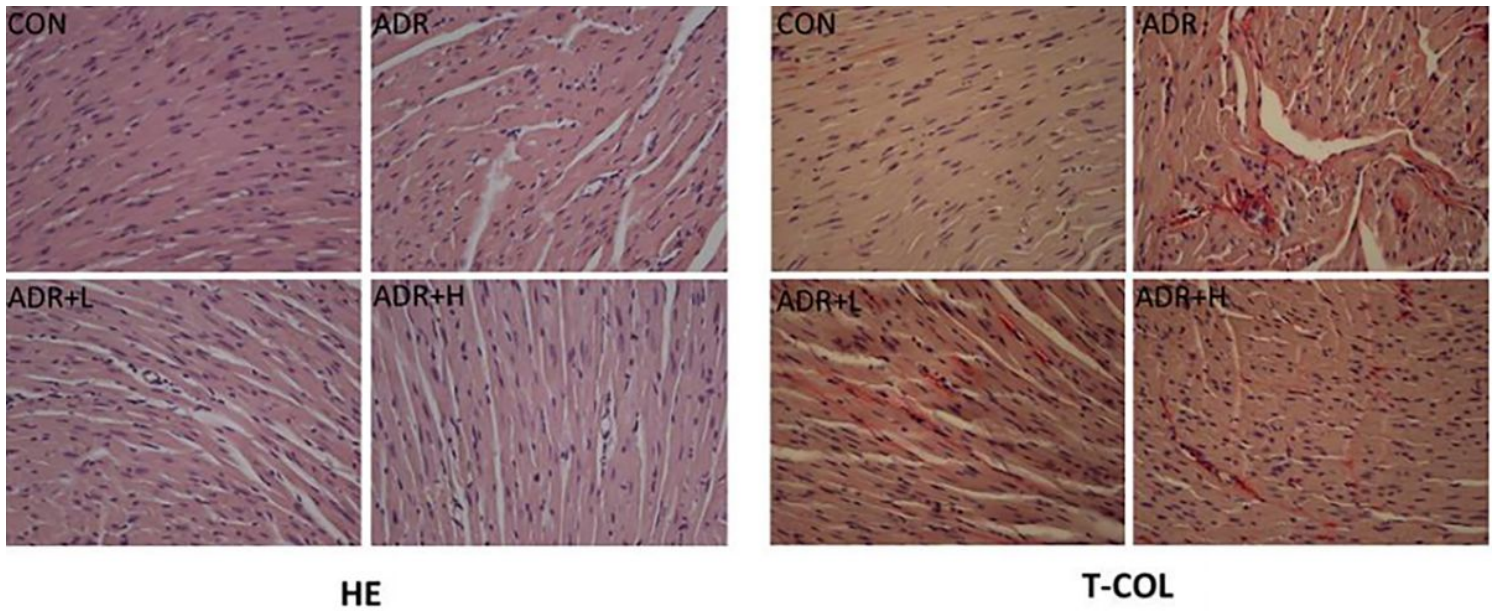


Figure 2

HE and T-COL staining of heart tissue. Representative micrographs of paraffin-embedded sections stained with HE and sirius red for total collagen, and photographed at a magnification of 400 \times .

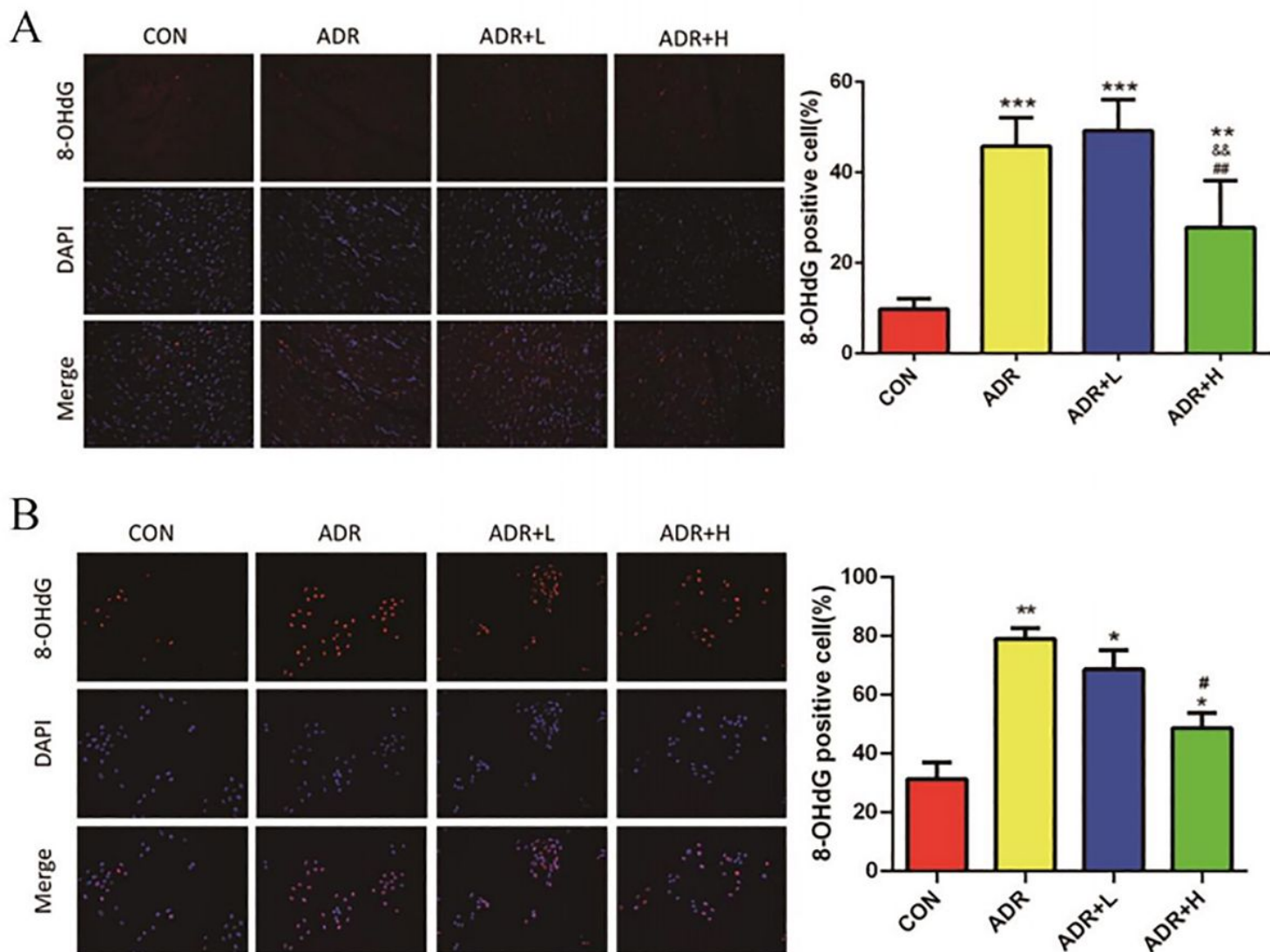


Figure 3

Myocardial DNA damage analysis Representative micrographs of immunofluorescence reaction for 8-OHdG, in vivo (A) and in vitro(B) photographed at a magnification of 400×. The percentage of positive cells were presented as the mean±SD. *P<0.05, **P<0.01, ***P<0.001 compared to CON group; #P<0.05, ##P<0.01, compared to ADR group; &&P<0.01 compared to ADR+L group.

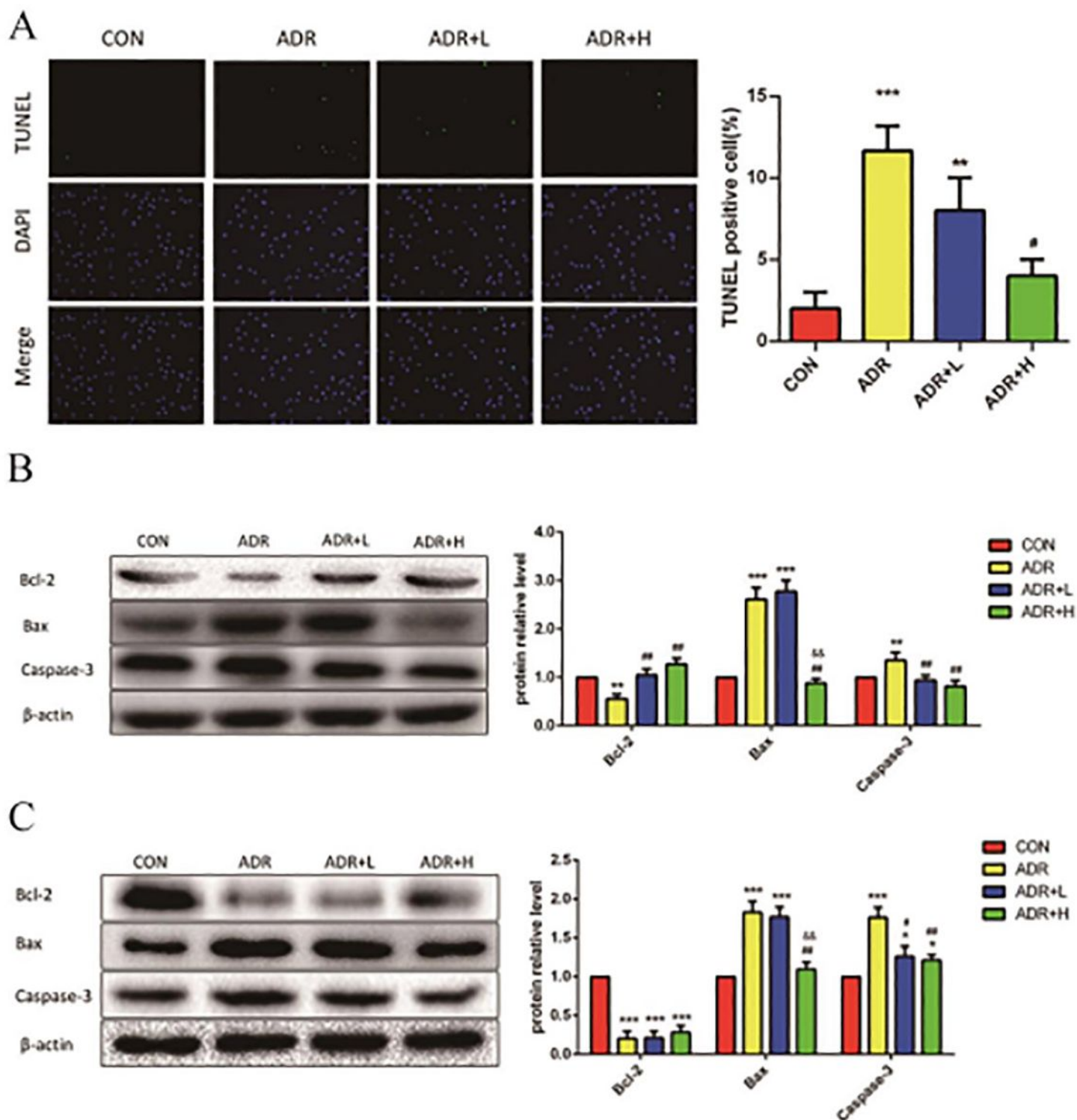


Figure 4

Myocardial apoptosis analysis (A) Representative micrographs of TUNEL staining, photographed at a magnification of 400 \times . The percentage of positive cells were presented as the mean \pm SD. Western blot analysis of Bcl-2, Bax and Caspase-3 protein expressions in vitro (B) and in vivo (C), β -actin was used as loading control. * P <0.05, ** P <0.01, *** P <0.001 compared to CON group; # P <0.05, ## P <0.01 compared to ADR group; && P <0.01 compared to ADR+L group.

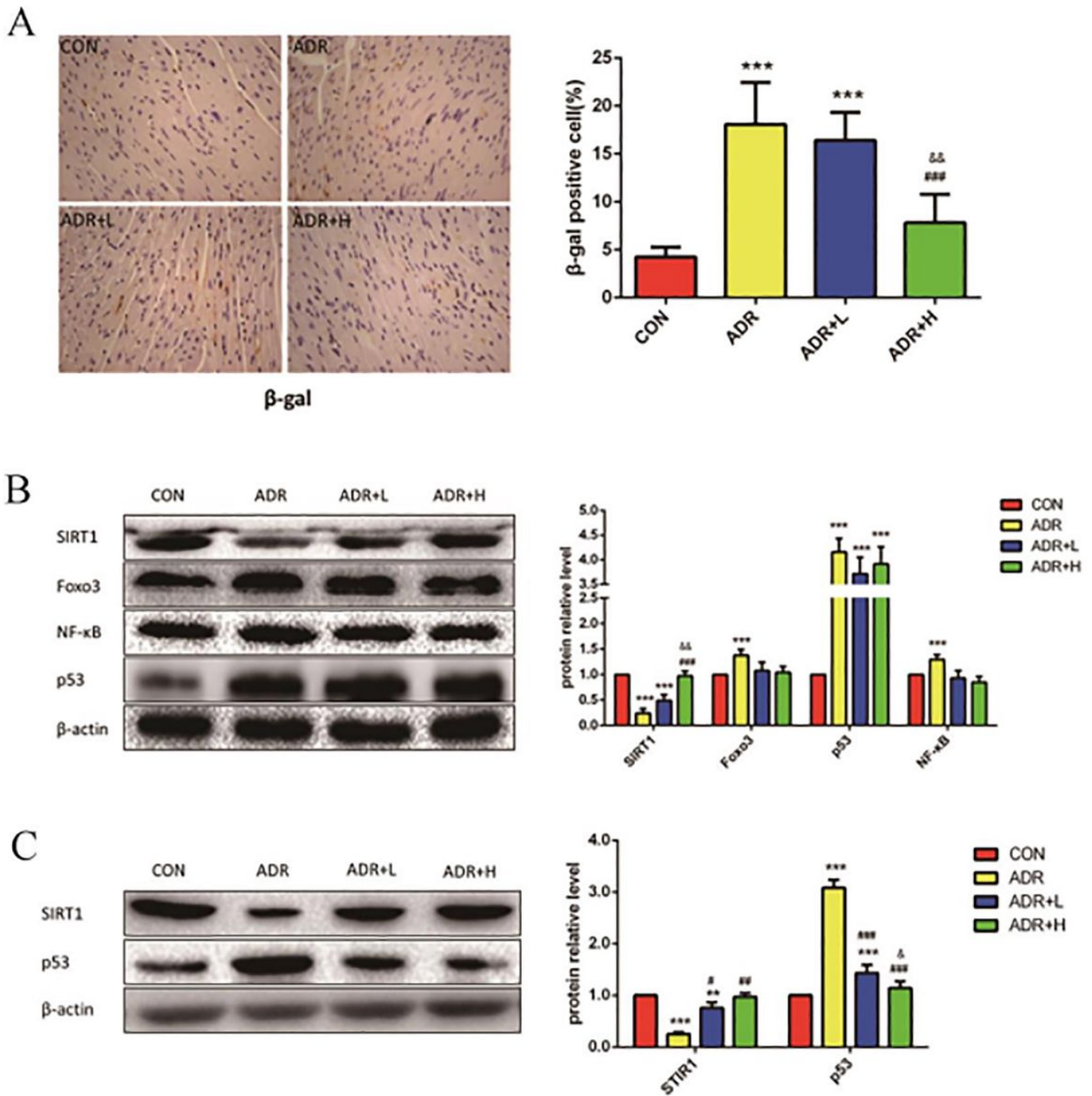


Figure 5

Myocardial senescence analysis (A) Representative micrographs stained with immunohistochemically for β -gal and photographed at a magnification of 400 \times . The percentage of positive cells were presented as the mean \pm SD. (B) Western blot analysis of SIRT1, Foxo3, p53 and NF- K B protein expressions and β -actin was used as loading control. (C) Western blot analysis of SIRT1 and p53 protein expressions in vitro and β -actin was used as loading control. **P<0.01, ***P<0.001 compared to CON group; #P<0.05, ##P<0.01, ###P<0.001 compared to ADR group; &P<0.05, &&P<0.01 compared to ADR+L group.

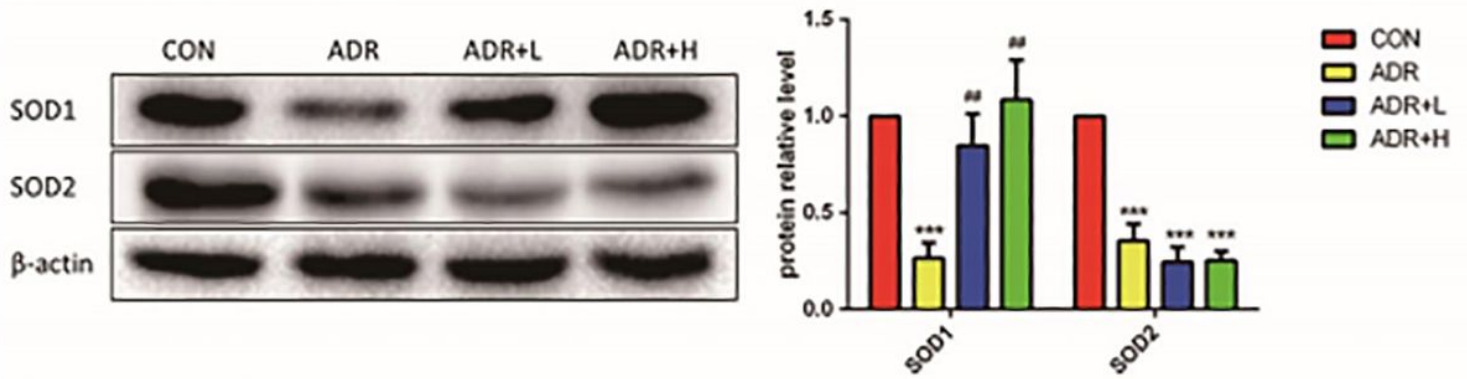


Figure 6

Oxidative stress levels changes Western blot analysis of SOD1 and SOD2 protein expressions and β -actin was used as loading control. *** $P < 0.001$ compared to CON group; ## $P < 0.01$, compared to ADR group.

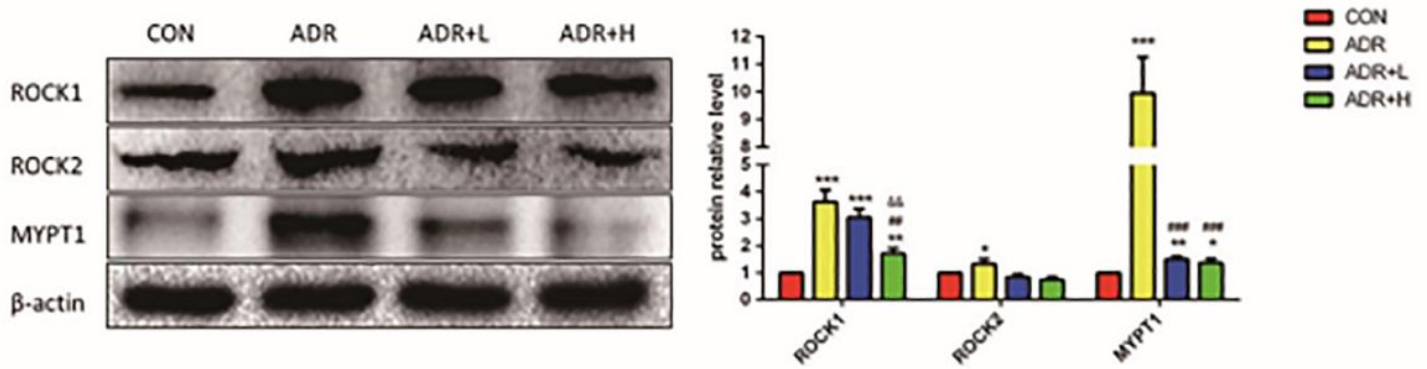


Figure 7

ROCK signaling pathway changes Western blot analysis of ROCK1, ROCK2 and MYPT1 protein expressions and β -actin was used as loading control. * $P < 0.05$, ** $P < 0.01$, *** $P < 0.001$ compared to CON group; ## $P < 0.01$, ### $P < 0.001$ compared to ADR group; && $P < 0.01$, &&& $P < 0.001$ compared to ADR+L group.